# RESEARCH ARTICLE | Building Neural Circuits: Wiring and Experience

Neuronal networks in the developing brain are adversely modulated by early psychosocial neglect

© Catherine Stamoulis, 1,2,3 Ross E. Vanderwert, Charles H. Zeanah, Nathan A. Fox, and Charles A. Nelson 1,4,7

<sup>1</sup>Harvard Medical School, Boston, Massachusetts; <sup>2</sup>Division of Adolescent Medicine, Boston Children's Hospital, Boston, Massachusetts; <sup>3</sup>Department of Neurology, Boston Children's Hospital, Boston, Massachusetts; <sup>4</sup>Division of Developmental Medicine, Boston Children's Hospital, Boston, Massachusetts; <sup>5</sup>Department of Psychiatry and Behavioral Sciences, Tulane University, New Orleans, Louisiana; <sup>6</sup>Department of Human Development and Quantitative Methodology, University of Maryland, College Park, Maryland; <sup>7</sup>Graduate School of Education, Harvard University, Cambridge, Massachusetts; and <sup>8</sup>School of Psychology, Cardiff University, United Kingdom

Submitted 9 January 2017; accepted in final form 4 July 2017

Stamoulis C, Vanderwert RE, Zeanah CH, Fox NA, Nelson CA. Neuronal networks in the developing brain are adversely modulated by early psychosocial neglect. J Neurophysiol 118: 2275–2288, 2017. First published July 5, 2017; doi:10.1152/jn.00014.2017.—The brain's neural circuitry plays a ubiquitous role across domains in cognitive processing and undergoes extensive reorganization during the course of development in part as a result of experience. In this study we investigated the effects of profound early psychosocial neglect associated with institutional rearing on the development of task-independent brain networks, estimated from longitudinally acquired electroencephalographic (EEG) data from <30 to 96 mo, in three cohorts of children from the Bucharest Early Intervention Project (BEIP), including abandoned children reared in institutions who were randomly assigned either to a foster care intervention or to remain in care as usual and never-institutionalized children. Two aberrantly connected brain networks were identified in children that had been reared in institutions: 1) a hyperconnected parieto-occipital network, which included cortical hubs and connections that may partially overlap with default-mode network, and 2) a hypoconnected network between left temporal and distributed bilateral regions, both of which were aberrantly connected across neural oscillations. This study provides the first evidence of the adverse effects of early psychosocial neglect on the wiring of the developing brain. Given these networks' potentially significant role in various cognitive processes, including memory, learning, social communication, and language, these findings suggest that institutionalization in early life may profoundly impact the neural correlates underlying multiple cognitive domains, in ways that may not be fully reversible in the short term.

**NEW & NOTEWORTHY** This paper provides first evidence that early psychosocial neglect associated with institutional rearing profoundly affects the development of the brain's neural circuitry. Using longitudinally acquired electrophysiological data from the Bucharest Early Intervention Project (BEIP), the paper identifies multiple task-independent networks that are abnormally connected (hyper- or hypoconnected) in children reared in institutions compared with never-institutionalized children. These networks involve spatially distributed brain areas and their abnormal connections may adversely impact neural information processing across cognitive domains.

Address for reprint requests and other correspondence: C. Stamoulis, Boston Children's Hospital, Division of Adolescent Medicine, 300 Longwood Ave., Boston, MA 02115 (e-mail: caterina.stamoulis@childrens.harvard.edu).

brain networks; EEG; early development; psychosocial neglect

FROM THE MICROSCALE of individual neurons to the macroscale of cortical regions, the brain's neuroarchitecture is characterized by networks organized into topologies that ensure flexible, rapid, and efficient neural information processing (Bullmore and Sporns 2009). These networks may be divided into two broad categories: task-related networks that are activated and coordinated in response to cognitive demands and external stimuli, and task-independent (resting-state or stimulus-independent) networks that are spontaneously active and coordinated when the brain is not actively engaged in specific cognitive tasks. In some cases, task-dependent networks increase their activity and coordination at the same time as specific task-independent networks decrease theirs (Fox et al. 2005). Thus, in part due to these inverse correlations, taskindependent networks may play a critical role in cognitive function and neural information processing (Dosenbach et al. 2008; Kelly et al. 2008; Raichle et al. 2001, Raichle and Snyder 2007). Predominantly fMRI studies in adults have identified several distinct, and in some cases interconnected task-independent networks, including the default-mode network (DMN) (Greicius et al. 2003; Mantini et al. 2007; Vincent et al. 2006; Ward et al. 2014). The topologies of these networks, estimated from fMRI data with excellent spatial resolution, may be directly correlated with those of structural networks (Barttfeld et al. 2015; Greicius et al. 2009). Previous studies have associated disrupted task-independent networks, with neuropsychiatric disorders, including schizophrenia and autism (Bluhm et al. 2007; Kennedy et al. 2006).

The dynamic evolution of task-independent networks in the developing brain is poorly understood and our current knowledge is primarily based on fMRI studies. Elements of these networks come on line early in infancy (Fransson et al. 2007), but at least the DMN, which includes the ventral medial prefrontal cortex, anterior cingulate cortex, posterior cingulate cortex, lateral temporal cortex, precuneus and lateral parietal inferior gyri, and the hippocampal formation (Buckner et al.

2008; Greicius et al. 2003), may be incompletely connected even at ages 7-9 yr (Fair et al. 2008). Negative early experiences and stressors, including poverty, abuse, and psychosocial neglect, may have profound effects on neural maturation and consequently brain structure and function. In fact, social and emotional deprivation associated with institutional rearing has been shown to adversely affect brain's structure (Bauer et al. 2009; Bick et al. 2015; Eluvathingal et al. 2006; Sheridan et al. 2012), metabolism (Chugani et al. 2001; Tottenham et al. 2011) and electrical activity (Marshall et al. 2004, 2008; McLaughlin et al. 2010, 2011; Stamoulis et al. 2015a; Vanderwert et al. 2010). Earlier work on the Bucharest Early Intervention Project (BEIP), a longitudinal study of children with a history of severe early deprivation (see Nelson et al. 2014; Zeanah et al. 2003), has shown that early psychosocial deprivation significantly impacts age-related dynamics in the developing brain's rhythms (Stamoulis et al. 2015a). In the same sample, Marshall et al. (2008) showed that removal from an institution and placement in a foster care home before 24 mo of age resulted in higher local network synchrony and statistically higher power in the alpha band (8–12 Hz) in the first 4 yr of life in comparison to children who remained in institutions. A positive modulatory effect of foster care placement was also reported in other oscillations (Stamoulis et al. 2015a), although changes in these oscillations from 42 to 96 mo were found to be distinct in children removed from institutions and placed in foster care compared with those who had never been institutionalized. These results highlight the profound adverse effects of early institutionalization on the developing brain.

There are very few studies that have investigated taskindependent networks in the developing brain and no previous work on the effects of neglect on these networks. This study investigated the topologies of task-independent networks and their developmental trajectories in children participating in the BEIP. Longitudinal electrophysiological (EEG) data from three cohorts were analyzed, including a group of institutionalized children who were randomized to a high-quality foster care placement (the foster care group), a group randomized to remain in institutional care (care as usual group) and a group of children who had never been institutionalized and lived with their families in the Bucharest community (never-institutionalized group). Although EEG has excellent temporal resolution, it lacks the high spatial resolution of fMRI and cannot resolve network topologies with the same spatial specificity as fMRI. Consequently, brain network topologies estimated from fMRI (which measures hemodynamic responses) and EEG (which measures neural activity) are not directly comparable. Nevertheless, EEG may still provide spatially sparse connectivity information on task-independent networks that may overlap with those identified by fMRI. Here we hypothesized that the spatial organization, properties and age-related dynamics of these networks are significantly impacted by early neglect in a frequency-specific manner, resulting in aberrant topologies that impair the efficiency of neural information processing and consequently cognitive function.

### MATERIALS AND METHODS

### Bucharest Early Intervention Project

The BEIP is an ongoing longitudinal study that started in 2001 as a randomized controlled trial with foster care as an intervention for

young children who had been abandoned at birth and placed in institutions. Using multimodal data, the study aims to investigate the effects of early psychosocial deprivation on the structure and function of the developing brain and potentially beneficial effects of removal from an institution and foster care placement (Nelson et al. 2014; Zeanah et al. 2003). One hundred thirty-six children who had been reared in institutions entered the trial at ages 6-30 mo and were randomized to two arms: care as usual (CAUG; n=68), i.e., more prolonged institutional rearing, and foster care (FCG; n=68), i.e., placement in high-quality foster care specifically created for the project. A comparison group of 72 Romanian children who had never been institutionalized and lived with their families in Bucharest communities was also recruited (NIG).

### **Participants**

The present study sought to quantify the age-related changes in task-independent networks using longitudinally acquired EEG signals from the BEIP cohorts, with an emphasis on 42 and 96 mo (although data at all ages were analyzed). Thus only subgroups of the BEIP cohorts with measurements at a minimum of two time points were included. Also, four children in the CAUG with diagnosed Autism Spectrum Disorder were excluded. The characteristics of these groups are described in more detail in (Stamoulis et al. 2015a). Sixty-two children in the CAUG [median age at study entry = 23.0 mo, interquartile range (IQR) = 9 mo], 61 children in the FCG (median age at study entry = 23.0 mo, IQR = 11 mo), and 44 children in the NIG (median age at study entry = 21.5 mo, IQR = 12 mo) were studied.

#### Demographic Data

Age, which varied between participants both at study entry and the second assessment (30-33 mo) but not at 42 or 96 mo, sex, age at foster care placement for children in the FCG, percent time spent in institutions for children in the FGC and CAUG, birth weight, and head circumference were included in the analysis as potential covariates. All missing data were assumed to be missing at random, mainly as a result of longitudinal attrition. Eighty-four girls and 83 boys were studied. Birth weight varied in the range 0.9-4.5 kg (median = 3.0kg, IQR = 0.8 kg). These data were missing in 15 children. There were no statistically significant differences in birth weight between the CAUG and FCG (median of CAUG = 2.8 kg, median of FCG = 2.6 kg, P = 0.14) but both groups had statistically lower birth weights than the NIG (median of NIG = 3.3 kg, P < 0.001). Head circumference was measured at all four time points. These data were missing for 17 children at baseline, 16 at 30 mo, 25 at 42 mo, and 32 at 96 mo. Median circumference at baseline was 46.8 cm, IQR = 2.5 moscm; 48.0 cm at 30 mo, IQR = 2.0 cm; 48.6 cm at 42 mo, IQR = 1.6cm; and 51.0 cm at 96 mo, IQR = 2 cm. There were no significant differences in head circumference between the CAUG and FCG at any age  $(P = 0.18 \text{ at baseline}, P = 0.07 \text{ at } 30 \text{ mo}, P = 0.09 \text{ at } 42 \text{ mo$ 0.38 at 96 mo). In the FCG, age at foster care placement was in the range 6.8-33 mo, median = 24.8 mo, IQR = 10.1 mo. Time spent at institutions at baseline, 42 and 96 mo is summarized in Table A1.

## EEG Data Characteristics and Preprocessing

EEGs were collected at study entry (baseline) as well as at 30–33, 42, and 96 mo, using an Electro-Cap (Electro-Cap International) system (12 scalp electrodes: F3, F4, Fz, C3, C4, P3, P4, Pz, T7, T8, O1, O2). The characteristics of these data are described in detail in (Marshall et al. 2008; Stamoulis et al. 2015a; Vanderwert et al. 2010). At baseline, 30–33 mo, and 42 mo assessments, task-independent EEG signals were recorded while lights were turned off for ~1–3 min. At 96 mo, task-independent EEG signals were recorded during 1-min intervals of eyes-closed (EC) and eyes-open (EO). Only signals recorded under the EC condition were included in the analysis. Data

were sampled at 512 samples/s and band-pass filtered during acquisition in the range 0.1- 100 Hz. Prior to analysis all signals were referenced to an average reference. Previous work has shown that in the absence of appropriate source modeling, which is difficult with a small number of electrodes, an average reference results in substantially lower connectivity errors than a mastoid or Cz reference (Chella et al. 2016). However, similar to all referencing approaches, an average reference has shortcomings, too, particularly for localizing specific EEG waveforms such as event-related potentials. Here, the issue of localization is of less concern. Also, several studies have shown that for connectivity analyses, even with a low number of EEG electrodes average referencing is preferable to the use of a common reference (Dien 1998). A stopband filterbank of third order elliptical filters with a 1-Hz bandwidth, 0.5 dB ripple in the passband, and 20 dB in the stopband was used to suppress the power line noise at 50 Hz and its 100-Hz harmonic. Artifacts associated with eye blinking were locally suppressed using a matched-filtering approach, where signal templates for eye blinks were used to detect intervals containing these artifacts (Stamoulis and Chang 2009). Individual EEG signals were further denoised via signal decomposition and elimination of random components identified based on their autocorrelation function (Stamoulis et al. 2015b). Finally, signals containing extreme amplitude outliers, i.e., above a threshold equal to the median plus three times the interquartile difference (Tukey 1977) were also eliminated. These outliers are likely to be associated with broadband muscle and/or other nonneural activity. Consequently, 1-s intervals containing outliers were excluded from the signal decomposition and mutual information estimations.

#### Signal Analysis

Estimation of narrowband EEG signal components (individual oscillations). Neural oscillations in the developing brain may have characteristic frequencies that do not fall within the limits of traditional biological bands (delta to ripple), established based on adult brain signals. Thus frequency domain analysis of band-pass-filtered signals in these bands may not be appropriate. Instead, a fully unsupervised, time-domain approach based on the Ensemble Empirical Mode Decomposition method (EEMD; Wu and Huang 2009) was used to estimate neural oscillations and their dominant frequencies. The EEMD is a modification of the classical Empirical Mode Decomposition method (Huang et al. 1998) and accounts of the problem of mode (component) mixing. The estimation process has been described in detail in previous work (Stamoulis et al. 2015a). Task-independent network connectivity was estimated for individual oscillations of the EEG to construct frequency-specific networks. Briefly, each EEG signal was decomposed into a small set of narrowband components that significantly contributed to the broadband signal amplitude. The cost function proposed by Stamoulis and Betensky (2011) was also used to select nonrandom components and eliminate noise-related signal contributions with substantial amplitude. A sliding 1-s window was used in all estimations. In exploratory analyses of the data, the window length was varied between 1 and 4 s, yielding similar estimates in oscillation amplitude, frequency, and connectivity.

Glossary of terms. The following network parameters were estimated for each identified oscillation in the EEG: 1) spatially averaged connectivity (over the entire brain and over individual networks identified in models to be statistically distinct between groups), 2) nondirectional edge-specific connectivity for each edge connecting pair of network nodes, and 3) node centrality, a measure of the importance of each node in the network. Each electrode was treated as a network node. Spatially averaged and edge-specific connectivities were quantified using mutual information, an information theoretic measure (see Estimation of oscillation-specific connectivity section). Two types of connectivity matrices were estimated for each child at each time point and each oscillation: a weighted connectivity matrix containing the actual mutual information values and thus the actual

connection strengths between pairs of nodes and the adjacency matrix, a binary matrix of edge connection/nonconnection obtained by appropriately thresholding the weighted connectivity matrix. Based on connectivity thresholds two sets of networks were identified, hyperand hypoconnected networks (see *Connectivity threshold estimation* and *Adjacency matrix estimation for relative hyper- and hypoconnectivity* sections). Node centrality was quantified using node strength, a measure of the sum of its connections based the adjacency matrix (see *Estimation of node centrality* section).

Estimation of oscillation-specific connectivity. In the case of a large number of electrodes, connectivity analysis may be best conducted at the source level, to appropriately address issues of volume conduction that may impact various connectivity measures. The adequacy and accuracy of source connectivity analysis in the case of 12 electrodes are questionable, independently of the source separation or localization methods used. Information-based connectivity measures have been shown to be relatively robust to volume conduction (Vicente et al. 2011) and were used in this electrode-level analysis. Mutual information was used to quantify undirected pairwise network connectivity. Together with other information theoretic measures, it has been previously used in a number of studies to quantify correlation between electrophysiological signals and may be more robust to the inherent noise of these signals than other measures such as coherence (Palus et al. 2001; Schreiber 2000; Stamoulis et al. 2013; Vejmelka and Palus 2008). Mutual

information  $I(X,Y) = \sum_{x,y} p(x,y) \log \frac{p(x,y)}{p(x)p(y)} \ge 0$ , between random variables X and Y, measures their mutual dependence (Cover and Thomas

ables X and Y, measures their mutual dependence (Cover and Thomas 2006). It is a function of their joint and marginal probability density functions p(x, y), p(x), and p(y), which were estimated using a kernel-based method (assuming a Gaussian kernel) following segmentation of EEG signals in 1-s windows. Across ages and participants, a kernel bandwidth of 0.8 was used in the estimation and the probability density functions were evaluated at 200 points.

Connectivity threshold estimation. Edge-specific mutual information thresholds were estimated as follows: for each oscillation and network edge, the median (across subjects) mutual information for the NIG (and thus each age-matched oscillation and edges in the control group) was calculated as well as corresponding 95% confidence intervals (CI), using bootstrapping with replacement [2,000 draws and an accelerated, bias-corrected percentile method (Efron and Tibshirani 1993)]. The edge-specific upper CI for the NIG median mutual information was selected as an edge's threshold for edge hyperconnectivity, and the corresponding lower CI was selected as the threshold for edge hypoconnectivity.

Adjacency matrix estimation for relative hyper- and hypoconnectivity. Based on the above thresholds, two sets of adjacency matrices, with elements (i, j) for edges connecting nodes i and j, for each oscillation-specific undirected graph, were estimated for the CAUG and FCG: I) the hyperconnectivity adjacency matrices, with elements that were equal to 1 for edges that exceeded the upper CI for median connectivity of the NIG and zeros elsewhere, and 2) the hypoconnectivity adjacency matrices, with elements that were equal to 1 for edges that were below the lower CI for median connectivity of the NIG and 0 elsewhere.

Estimation of node centrality. The maximum number of possible connections of each node in the estimated networks is 12 (a self-connection and 11 connections to all other nodes). There are several ways to define node centrality, i.e., the importance of a node in a network. Here it is defined in two ways: 1) in terms of node strength, i.e., the ratio of the sum of all edge weights for a node over the

maximum possible sum of weights, so for node  $c_i = \frac{\sum_j I_{ij}}{\max \sum_j I_{ij}}$ ; and 2) in terms of node connectedness, i.e., the ratio of the sum of all binary edge values for a node over the maximum possible sum of

binary edge values for a node over the maximum possible sum of weights, i.e.,  $c_i = \frac{\sum_j A_{ij}}{max \sum_j A_{ij}}$ . Based on these topological measures it

is possible to identify potential hubs, i.e., highly connected nodes that are critical for information processing through the network. Note that the adjacency matrices for the CAUG and FCG were estimated as described above. The adjacency matrices for subjects in the NIG were estimated assuming the median (across subjects and electrodes) mutual information as the corresponding connectivity threshold.

#### Statistical Analysis

Differences in network characteristics at individual ages were assessed using ordinary linear regression models, with edge connectivity or node centrality as the dependent variable, and group (using criterion coding to avoid including several group variables given the relatively small sample), time spent in institutions, birth weight, head circumference, age at foster care placement, and sex (categorized as female = 0, male = 1) as independent variables. In individual models (ordinary or mixed effects models used to assess age-related parameter changes), each edge or node parameter was assessed independently of each others, although part of a network and thus effectively correlated. Corrections for multiple comparisons were not necessary, particularly in mixed effects models (Gelman et al. 2012). Combinations of independent variables were included in separate models. Logistic regression models with group as the dependent variable (assuming the NIG as the reference category) and network measures as independent variables were also developed. Finally, in cases where network parameters were found to be statistically distinct among the three groups, their relationship was also investigated through logistic regression models that included only the CAUG (=0) and FCG (=1), i.e., the groups in the two arms of the randomized trial. All modeling approaches yielded consistent results. Note that at baseline (before the randomization) there were only two groups: institutionalized and never-institutionalized.

Linear mixed-effects models were developed to investigate temporal trajectories of network characteristics. For all children randomized to the intervention arm, foster care placement occurred before 42 mo of age. Therefore, to assess intervention-related effects we focused on changes in network parameters between 42 and 96 mo. Thus the models included a subject-specific intercept and a subject-specific age slope, to account for potential subject-specific variabilities. Independent variables included sex, birth weight, head circumference, group, age at foster care placement, and percent time spent at institutions. Given the sample size, only relatively small models were developed with combinations of 1–3 independent variables. All analyses were done using the software MATLAB (MathWorks, Natick, MA).

### RESULTS

We investigated oscillation-specific network properties at all four age assessments and their developmental changes from 42 to 96 mo. We first examined spatially averaged (global) connectivity followed by edge-specific connectivity and node centrality. We conducted two complementary analyses: 1) Using connectivity thresholds derived from the NIG, we compared the FCG and the CAUG relative to NIG. We thus present results on abnormal networks in the FCG and CAUG that were found to be hyperconnected or hypoconnected relative to the NIG; and 2) we compared all three groups to each other via statistical models that included adjustments for birth weight or head circumference. We report network measures only for subnetworks that were found to be statistically distinct in the three groups. As previously noted, regression models were also developed to compare only the CAUG and FCG, separately from the NIG. Statistically significant group differences in network parameters identified in these models were consistent with those identified using models that included the NIG.

Brainwide (Spatially Averaged) Connectivity

First, median (over electrodes) mutual information that had been averaged in time was compared between groups for each estimated oscillation at each assessment age, to assess potential differences in brain/hemisphere-wide connectivity. Corresponding frequency-connectivity relationships at these ages (unadjusted for confounders or other covariates) are shown in Fig. 1. Interquartile ranges (vertical bars for mutual information and horizontal bars for frequency) are shown. In these unadjusted connectivity data, no significant differences were found between groups except for the gamma oscillation at 96 mo (P = 0.012), and the alpha and theta oscillations at baseline (study entry) (P = 0.002 and P = 0.016 for alpha and theta connectivity, respectively). When adjusted for birth weight or head circumference, significant differences in whole brain and hemisphere-specific connectivity were estimated between institutionalized and never-institutionalized children in the theta band at baseline (P = 0.006 for the entire brain, P = 0.002 for the left hemisphere and P = 0.034 for the right hemisphere). When adjusted for age at foster care placement, significant group differences in left-hemisphere theta connectivity were estimated at 96 mo (P = 0.035). When adjusted for head circumference, significant group differences in beta connectivity were also estimated in the left hemisphere at 96 mo (P =0.044). The statistics of oscillation frequencies at each assessment age are summarized in Table A1 in the APPENDIX.

### Network Topologies at Four Assessment Ages

All reported connectivity parameters in the CAUG and FCG are relative to the corresponding NIG parameters. For each assessment age and oscillation, network topologies for the two groups are shown in Fig. 2. Note that these connectivities are unadjusted for potential confounders and are solely based on thresholding of the mutual information matrices. Appropriate adjustments were included in the analysis and are described in the next section. For each oscillation, topologically distinct hyper- and hypoconnected subnetworks were identified in the CAUG and FCG with some overlap of their elements across oscillations. At baseline, both groups had a large number of hyperconnected edges (up to ~85% of all possible edges) and a small number of hypoconnected edges. This number decreased significantly from baseline to the second assessment (from more than 75% to ~25% of all possible connections), potentially due to neural maturation and elimination of redundant connections. No substantial topological differences were estimated between the two groups at those ages. At 42 mo, an even lower number of hyperconnected edges were identified in both groups, asymmetrically clustered in the left hemisphere and primarily in temporoparietal and parieto-occipital regions in the gamma and beta networks, but less consistently (in space) in other networks. For some oscillations, a small number of hypoconnected edges were also identified. Finally, at 96 mo, more consistent topologies were identified in both groups: 1) a hyperconnected gamma network with aberrant connections between bilateral parietal and occipital regions and 2) relatively larger hypoconnected beta and alpha networks with aberrant connections primarily between left and right temporal regions, left temporal and bilateral frontal and occipital regions.

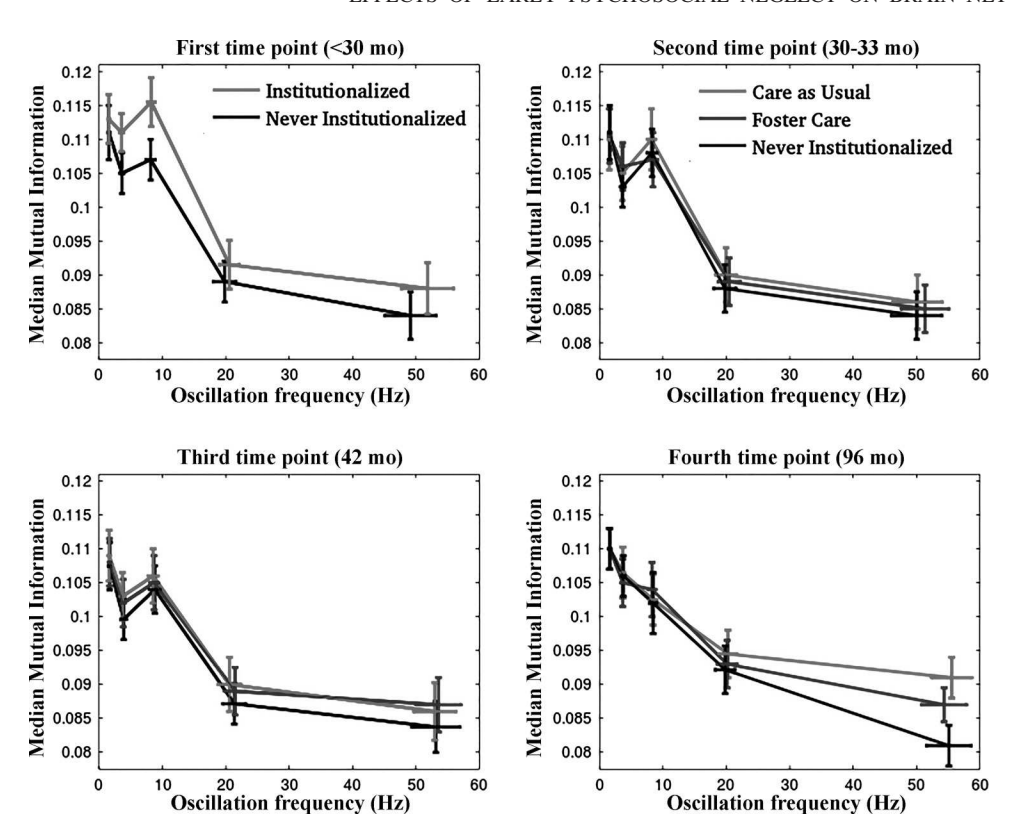


Fig. 1. Frequency-connectivity (measured by mutual information) plots for all estimated oscillations at baseline (top left), and clockwise at ~30–33, 42, and 96 mo, respectively. At the first 3 time points connectivity was estimated from task-independent EEGs under the lights off recording condition and at 96 mo under the eyes-closed condition. The 3 groups are superimposed: Care as Usual group (CAUG), Foster Care group (FCG), and Never-institutionalized group (NIG). At baseline, and thus before randomization, children in the CAUG and FCG were part of the Institutionalized group.

Network Topologies and Parameters at 42 and 96 mo

To validate the findings of the above threshold-based analysis and include appropriate adjustments for potential confounders, all three groups were explicitly compared at 42 and 96 mo using statistical models. Statistically distinct networks based on the models are shown in Fig. 3. No significant sex effects were found in any parameter at any age  $(P \ge 0.40)$ .

### Network connectivity

Forty-two months. Although the above threshold-based analvsis identified statistically distinct edges between the NIG and both the CAUG and FCG, when adjusted for birth weight or head circumference at that age in the models, no statistically distinct edges were identified between the three groups. The effect of age at foster care placement was found to be significant for right frontocentral (F4, C4) and centroparietal (C4, P4) regions in the gamma networks, with statistically higher connections in the CAUG followed by the FCG and the NIG (P = 0.007, Wald statistic = 7.74 for group, P = 0.006, Wald)statistic = 7.63 for age at foster care placement). Connectivity between occipital regions was also statistically higher in the CAUG followed by the FCG and the NIG and in the alpha and theta networks (P = 0.013, Wald statistic = 6.39 for group, P = 0.027, Wald statistic = 5.04 for age at foster care placement in the alpha network, and P = 0.030, Wald statistic = 4.87 for group, P = 0.047, Wald statistic = 4.07 for foster care placement in the theta network).

*Ninety-six months*. The majority of aberrantly connected edges identified by the threshold-based analysis were also found to be distinct in the three groups through the statistical models. For oscillations in the gamma to theta ranges, statistically distinct subnetworks/edges and corresponding brain

regions are summarized in Table 1. Related model statistics for these edges and subnetworks are summarized in Table A3. Adjustments for birth weight and age at foster care placement were nonsignificant in all models (P>0.17 for birth weight and P>0.06 for age at placement). Similarly, the adjustment for head circumference was nonsignificant for all models for gamma connectivity (P>0.2), all models for beta connectivity with the exception of the (F3, T7) connectivity (P=0.047) and marginally for the (F4, T7) connectivity (P=0.056), all models for alpha connectivity with the exception of the (P3, P2), (P4, Pz) and (T7, 02) connectivities (P=0.028, P=0.019 and P=0.030, respectively), and all models for theta with the exception of the (P3, P4) connectivity (P=0.020 for theta). Median mutual information for each group is shown in column 2.

Within the gamma network, the parieto-occipital subnetwork (P3, Pz, P4, O1, O2, and averaged connectivity in this subnetwork) was found to be statistically distinct in the three groups with highest connectivity in the CAUG followed by FCG. Elements of this subnetwork were also hyperconnected across frequency ranges.

In the beta network, the left temporal region (T7) in the CAUG and FCG was statistically hypoconnected to several other brain regions, including bilateral frontal (F3, Fz, F4), right temporal (T8), bilateral parietal (P3, Pz, P4), bilateral occipital (O1, O2), and right central (C4). These connectivities, as well as averaged connectivity in the corresponding subnetwork were distinct in the three groups, with statistically lowest values in the CAUG. We examined the raw signal from electrode T7 across subjects to ensure that the observed laterality of these aberrant connectivities was not associated with artifacts or noise. No significant signal variance differences were found between groups or subjects. All hypoconnections

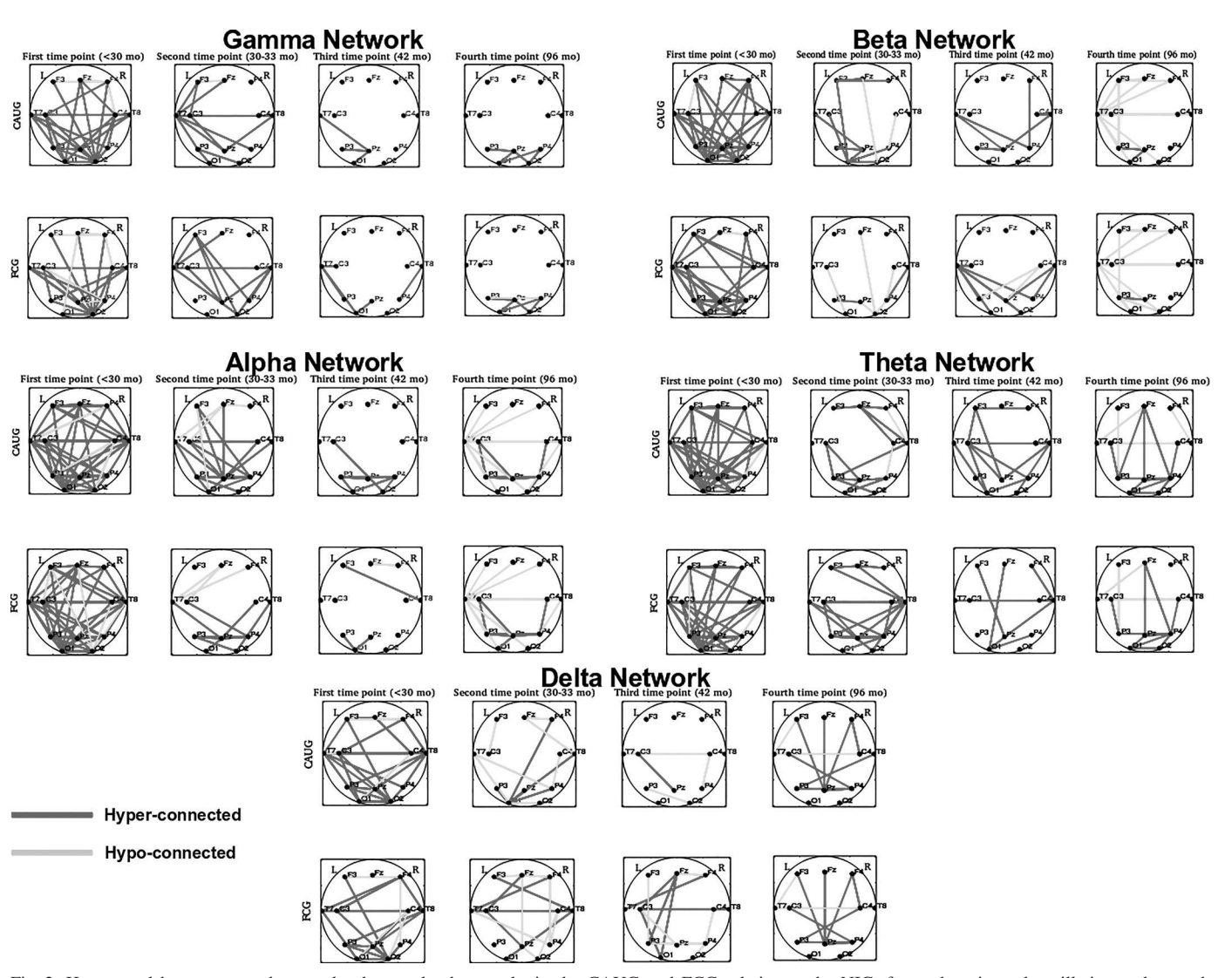


Fig. 2. Hyper- and hypoconnected network edges and subnetworks in the CAUG and FCG relative to the NIG, for each estimated oscillation and at each assessment age (baseline to 96 mo from left to right). Edges with mutual information (MI) values higher than the upper MI threshold are marked in dark gray, and edges with MI values below the lower MI threshold are marked in dark gray.

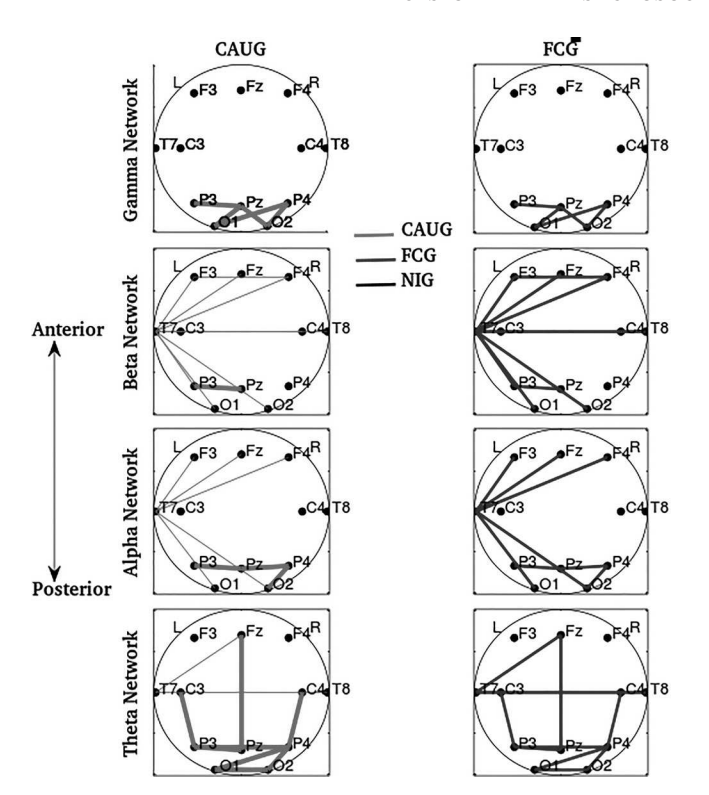
from the beta network were also found to be distinct between groups in the alpha network, with the exception of bilateral frontal, bilateral temporal and the right central–left temporal connections. Averaged connectivity in this subnetwork was also found to be statistically lowest in the CAUG. In the theta network, frontoparietal (Fz, Pz), bilateral centroparietal (C3, P3) and (C4, P4), and most edges of the aberrant gamma subnetwork were statistically distinct between groups, with highest connectivities in the CAUG followed by the FCG. Also, elements of the hypoconnected beta subnetwork were distinct in the three groups, with lowest connectivities in the CAUG. Finally, centroparietal connections in the theta network were also found to be statistically distinct between groups in the delta network, with highest connectivities in the CAUG.

# Node Centrality

A few nodes with statistically distinct connectedness across the three groups were found both at 42 and 96 mo and are summarized in Tables 1 (96 mo) and A4 (both ages). At 42 mo, these included T7 in the gamma network; Fz, T7, and T8 in the

beta network; Pz in the alpha network; and Fz and Pz in the theta network. At 96 mo, Pz had the highest connectedness in all networks except delta, similarly for C3, C4, and P4 but only in the beta and alpha networks and Fz in the theta network. T7 had the lowest connectedness in the beta and alpha networks. We examined the raw signals in electrode Pz across subjects to ensure that increased connectedness was not due to spurious correlations between signals. No significant signal differences were found between this and other electrodes. Birth weight, head circumference, and age at foster care placement all had nonsignificant effects (P > 0.08 for birth weight, P > 0.13 for head circumference, and P > 0.05 for age at foster care placement).

A subset of nodes with distinct connectedness among groups also had distinct node strengths but only at 96 mo. The statistics of corresponding models are summarized in Table A5. Similarly to connectedness, node Pz had statistically higher strength in the CAUG in the gamma, beta, and alpha networks and node T7 the lowest strength in the beta to delta networks. Nodes F3, F4, Fz, and T7 all had the lowest strengths



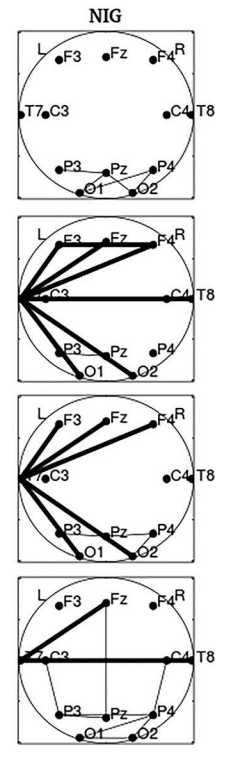


Fig. 3. Oscillation-specific network edges for which connectivity was statistically distinct in the 3 groups, adjusted for birth weight and head circumference at each age. Left plots correspond to the CAUG, middle to the FCG, and right to the NIG. Distinct line widths represent differential median (across the group) mutual information values, with thickest lines representing the highest median connectivity among groups and the thinnest lines representing the lowest connectivity.

in the CAUG followed by the FCG in the beta network. Finally, P4 was also found to have statistically distinct strength in the three groups both in the alpha and theta networks, with highest strength in the CAUG. Birth weight and age at foster care placement had nonsignificant effects in all networks and nodes ( $P \ge 0.09$  for both), and head circumference also had a nonsignificant effect ( $P \ge 0.08$ ) except for node P4 in the alpha network (P = 0.016). The spatial distribution of all nodes with distinct strengths in gamma, beta, alpha, and theta networks is shown in Fig. 4. In addition to edges that were distinct between groups (those of Fig. 3), edges that exceeded the median (over subjects) NIG connectivity but were not significantly different between groups are also superimposed (dashed lines). Independently of significance, a higher number of connections were estimated in the CAUG followed by FCG across oscillations. In summary, a few nodes in previously identified distinct subnetworks among groups were found to be either aberrant hubs or to have abnormally low centrality in the CAUG and FCG, suggesting additional topological differences between these groups.

# Network Parameter Trajectories from 42 to 96 mo

All previous analyses investigated network properties at individual assessment ages. To assess the impact of early neglect on the development of these networks, we also investigated the age-related changes in estimated parameters from 42 to 96 mo using appropriate statistical models for repeated measures.

# Connectivity Trajectories

For each oscillation, the changes in all network edges were estimated and compared between groups, using mixed effects regression models that included time (age), group, and birth

Table 1. Summary of aberrantly connected and statistically distinct network elements (edges and nodes) in the three groups

Oscillation/	Edge	e Connectivity	ntrality	
Network	Hyperconnected	Hypoconnected	Highest	Lowest
Gamma range (52.0–57.0 Hz)	Regions: Parietal; Parieto-occipital Edges: P3-Pz; P4-O1, O2; Pz-O1, O2		Pz	
Beta range (20.0–23.0 Hz)	Regions: Parietal	Regions: Left temporal; Bilateral frontal; Parietal; Occipital	Pz, C3, C4, P4	T7, F3, F4, Fz
	Edges: P3-Pz	Edges: T7-F3, Fz, F4, C4, P3, Pz, P4, O1, O2; F3-F4; T7-T8		
Alpha range (8.0–10.0 Hz)	Regions: Parietal; Parieto-occipital	Regions: Left temporal; Bilateral frontal; Parietal; Occipital	Pz, C3, C4, P4	T7
	Edges: P3-Pz, P4-Pz, P4-O2	Edges: T7-F3, Fz, F4, C4, P3, Pz, P4, O1, O2		
Theta range (3.6–4.3 Hz)	Regions: Midline; Centroparietal; Parietal; Parieto-occipital Edges: Fz-Pz, C3-P3, C3-P4, O1-O2, P3-P4, P4-O1, P4-O2, P3-Pz	Regions: Left, bilateral temporal; Bilateral Centroparietal; Parietal; Occipital Edges: Fz-T7, Pz; C3-P3, C4-P4, P3-Pz, P4; P4-O1, O2; T7-T8; O1-O2	Pz, Fz, C3, C4, P4	Т7

For each oscillation frequency range, hyper- and hypoconnected brain regions and sets of network edges as well as aberrantly connected nodes (based on their centrality estimated either as node strength or connectedness) are listed.

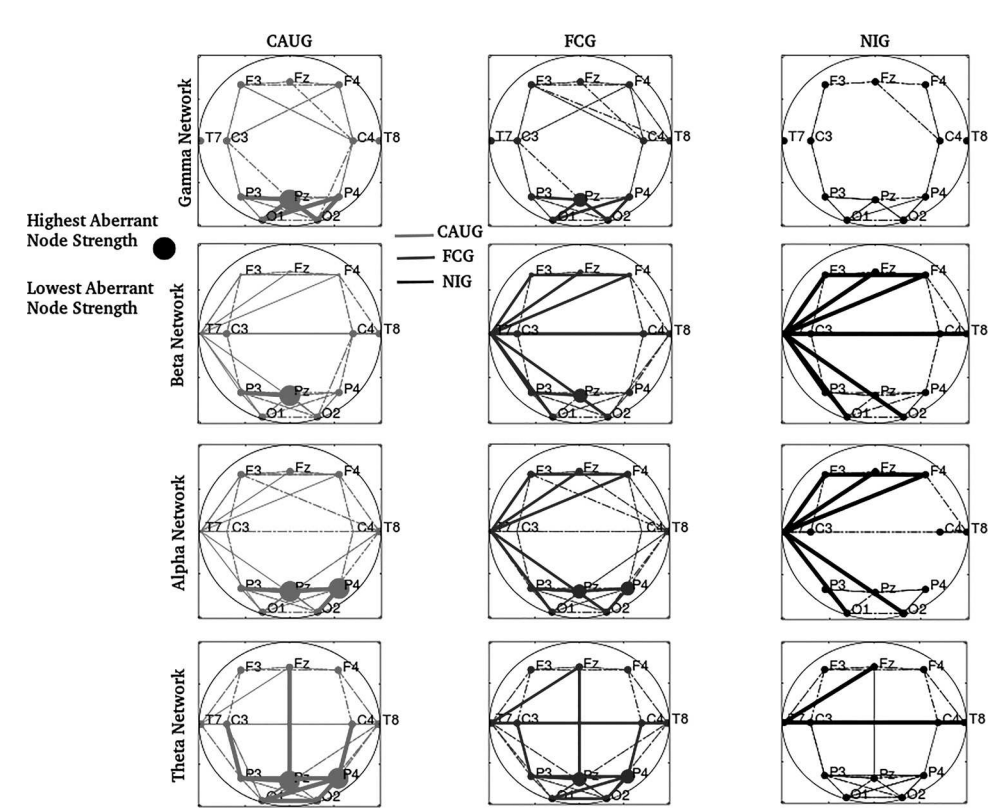


Fig. 4. Network nodes with aberrant strength (centrality) across groups, in the gamma, beta, alpha, and theta networks. Larger circles and thicker lines reflect aberrantly and significantly higher node strength and connectivity (edge weight). Dashed lines correspond to edges above the NIG median connectivity threshold, which were not, however, statistically distinct between groups.

weight or head circumference (and/or age at foster care placement) as independent variables and pairwise mutual information as the dependent connectivity variable. The statistics of these models for edges that were distinct between groups are summarized in Table A6. The effect of time (age) was significant in all these models ( $P \le 0.01$ ). Birth weight and head circumference had nonsignificant effects in all models (P > 0.17 for birth weight, P > 0.26for circumference). A small number of network connections had distinct age-related changes across groups, including (P3, Pz) and (P4, O2) across oscillations except delta, and (C3, P3), (P3, O2), (P4, O1), and (Pz, O2) in the gamma network. Note that with the exception of (C3, P3) these edges were also found to be distinct at 96 mo and were part of the parieto-occipital hyperconnected subnetwork in the CAUG and FCG compared with NIG.

### Node Centrality

With the exception of node P3 in the gamma network with marginally significant age-related changes across groups (P=0.053, Wald statistic = 3.77) no other node strength changed significantly from 42 to 96 mo. However, connectedness in nodes P4 and Pz in the alpha and theta networks changed in a statistically distinct way across groups. Both nodes belong to the subset of nodes with distinct connectedness at 96 mo in the three groups (Pz also had statistically distinct connectedness at 42 mo; see Table A7). Birth weight and head circumference had nonsignificant effects (P>0.21 for birth weight, P>0.05 for head circumference). These results suggest that at least elements (nodes and edges) of task-independent networks develop abnormally as a function of age in children reared in institutions, resulting in significant differences at 96 mo.

#### DISCUSSION

In this paper we report the impact of early psychosocial deprivation associated with institutionalization on the topologies and age-related dynamics of frequency (oscillation)-specific, task-independent brain networks in three groups of children from the BEIP. To investigate these topologies, we have used multiple statistical modeling approaches and network measures. Our present findings extend previous work (Stamoulis et al. 2015a), which has shown that early institutionalization has profound and widespread effects on broadband neural activity.

In children reared in institutions and thus subjected to early neglect, this study has identified two aberrantly connected networks, particularly at 96 mo: 1) The aberrantly hyperconnected parieto-occipital gamma network in the CAUG and FCG, both with statistically higher connectivity than the NIG, but also with distinctly different connectivity from each other. Elements of this subnetwork were also aberrantly hyperconnected at lower frequencies (beta, alpha, and theta networks). 2) The hypoconnected frontotemporal network at frequencies below the gamma range (beta to delta) in the CAUG and FCG compared with NIG at 96 mo, but also distinctly different from each other. Although the adverse effects of early stressors on neural maturation and the development of human brain networks remain elusive, there is substantial evidence that brain development is significantly impacted by early experiences (Nelson et al. 2006). Therefore, negative experiences may significantly and differentially affect the maturation of the brain's neural circuitry, impairing both selective connection strengthening (leading to hypoconnected networks) and/or connection pruning (leading to networks that appear aberrantly hyperconnected at the macroscale). Both types of aberrant networks may prevent efficient neural information processing.

It is important to note the statistically lower connectivity in the FCG (although still statistically higher than NIG) compared with CAUG in the parieto-occipital network, suggesting a positive effect of the foster care intervention in lowering aberrant hyperconnectivity. Previous work has shown that this network is synchronized in the gamma band during visual processing (Helfrich et al. 2014). Abnormally high connectivity may imply reduced flexibility of this network to modulate its activity during visual task performance. In fMRI studies, elements of this network have been previously identified as major cortical hubs (Tomasi and Volkow 2011). Here, parietal nodes, which may overlap with this network, were found to be aberrant hubs at multiple frequencies, with abnormally high connectivities in the CAUG and FCG compared with the NIG. These regions are involved in a wide range of cognitive processes. For example, parietal regions are often activated during episodic memory retrieval (Cabeza et al. 2008) and are involved in self-projection (Buckner and Carroll 2007) as well as visuospatial processing (Tosoni et al. 2015). Furthermore, spatial attention has been shown to modulate the coordination between parietal and occipital regions during top-down processing of spatial attention information (Lauritzen et al. 2009). Thus abnormally high task-independent connectivity between these areas may adversely impact these cognitive processes.

Although elements of the hyperconnected parieto-occipital network had distinct connectivities in the three groups across frequencies, the largest number of aberrant edges in this subnetwork was estimated in the gamma frequency range. Gamma synchrony in parietal regions has been associated with visuomotor learning and object representation (e.g., Bertrand and Tallon-Baudry 2000; Perfetti et al. 2011; Galletti et al. 2003; Tallon-Baudry 2009). Previous studies have shown that children reared in institutions have decreased performance on tests of visual memory and attention (Bick et al. in press; Bos et al. 2009; Pollack et al. 2010), which may be explained by decreased flexibility in the underlying neural circuitry. At lower frequencies, particularly the theta and delta ranges, frontoparietal regions, which appeared to be aberrantly hyperconnected in the CAUG and FCG, have been shown to be part of a network that is characterized by spontaneous low-frequency activity and is anticorrelated with the DMN (Fox et al. 2005; Konrad and Eickhoff 2010), which implies that it should be weakly correlated at rest, in contrast to the DMN. Although neuronal networks identified in this study with low spatial resolution-EEG are not directly comparable with high-resolution fMRI networks, similar anticorrelations between taskdependent and task-independent networks may be measurable by both modalities. Therefore, aberrantly high task-independent connectivity in the identified parieto-occipital network may prevent suppression of its resting activity and inhibit its functional activation.

The second major finding of this study is the hypoconnected frontotemporal network at frequencies below the gamma range (beta to delta) in the CAUG and FCG compared with NIG at 96 mo. Several elements of this network may overlap with previously identified task-independent networks, e.g., the resting-state auditory-phonological and visual networks reported by Mantini et al. (2007). Left middle and transverse temporal regions, covered by electrode T7, were found to be significantly hypoconnected with bilateral frontal (F3, Fz, F4), bilat-

eral occipital (O1, O2), and right temporal (T8) regions. This node was also found to have statistically lower important (centrality) in the network in the CAUG and FCG. Left temporal regions are associated with hearing, language processing, and memory. The parietal-temporal-occipital association area is responsible for integrating visual and auditory information and is involved in language comprehension. Left frontotemporal connectivity has also been shown to be an essential network involved in syntactic processing (Papoutsi et al. 2011; Tyler et al. 2011). Note that spatially averaged connectivity in the left hemisphere was also found to be distinct in the three groups at 96 mo, in the beta and theta networks. Again, our findings may tap an underlying aberrant network associated with the behavioral evidence of impaired language development as a result of early institutionalization. It is important to note the distinct connectivity in this subnetwork in the CAUG and FCG, suggesting a positive effect of the foster care intervention in increasing connectivity in this subnetwork. Thus this change could be associated with the observed improvements in language learning as a result of the foster care intervention and age of that intervention (Croft et al. 2007; Windsor et al. 2011, 2013). A previous study of structural brain connectivity in the BEIP cohort (Bick et al. 2015) has shown impaired integrity of the corpus callosum in children reared in institutions, which would in part explain lower interhemispheric connectivity between temporal regions in the CAUG and FCG.

Although all network analyses in this study have consistently identified both the hyperconnected parieto-occipital network and the hypoconnected primarily left temporal network across several frequency bands at 96 mo, corresponding findings at 42 mo were less clear. A few elements of the parieto-occipital subnetwork with aberrant characteristics at 42 mo remained atypically connected at 96 mo, with distinct properties in the three groups. The dynamic trajectories of part of this subnetwork were also distinct among groups, potentially due to differential neural maturation rates. It is possible that additional network differences were difficult to detect at 42 mo due to incomplete and heterogeneous maturation of task-independent networks at this age, which could make it more difficult to detect connectivity group differences.

Finally, the frequency specificity of our findings varied between networks (e.g., a larger hyperconnected network in the gamma range compared with lower frequencies). Although higher-frequency networks imply spatially localized processing, lower-frequency oscillations facilitate the communication (or binding) between these networks. The presence of smaller numbers of aberrant connections at lower frequencies could in part be due to impaired binding between high- and lowerfrequency oscillations within corresponding networks. Our previous work has shown decreased coupling between taskindependent gamma and lower-frequency oscillations, which could in part explain these findings (Stamoulis et al. 2015a). Furthermore, substantial topological overlap between aberrantly hypoconnected edges were observed in the alpha and beta networks. Significant correlations between alpha and beta oscillations have been reported in task-independent EEGs, which may explain the topological similarities between the two networks (Carlqvist et al. 2005).

Despite its many methodological strengths (including its randomized control trial design), this study is not without

23, 2017

Table A1. Summary statistics of percent time since birth spent in institutions and corresponding time in months, for each group at baseline and 42 and 96 mo

Assessment Group	В	aseline	2	12 mo	96 mo	
	Median % time; Actual time, mo	(25th, 75th) quartiles	Median time; Actual time, mo	(25th, 75th) quartiles	Median time; Actual time, mo	(25th, 75th) quartiles
CAUG	98.6%	(81.6, 100.0) %	85.0%	(64.4, 97.1) %	53.0%	(36.2, 79.8) %
	19 mo	(16.9, 25.0) mo	35.7 mo	(27.0, 40.8) mo	50.9 mo	(31.2, 67.6) mo
FCG	95.9%	(69.4, 100.0) %	48.9%	(35.0, 61.8) %	23.40%	(18.3, 28.6) %
	18.3 mo	(16.3, 23.0) mo	20.5 mo	(14.7, 26.0) mo	22.5 mo	(15.0, 26.5) mo
NIG	0	0	0	0	0	0

limitations, including its relatively small sample size. Nevertheless, data from multiple time points were included in parts of the statistical analysis, and multiple statistical models were developed to compare the cohorts, all yielding consistent results, which supports the robustness of the findings. It is, however, possible that smaller network-level differences between groups were not detectable in this sample. Second, a small number of electrodes was used to record brain activity, which prevented appropriate source-level analyses to explicitly address the issue of volume conduction. However, information-based measures of connectivity were used in this study, which have been previously been shown to be relatively robust to volume conduction. Also, the low spatial resolution of the EEG limits the estimation of detailed network topologies possible by other modalities, particularly fMRI. Despite these limitations, to the best of our knowledge, this study provides the first evidence of multiple, significantly impacted, and aberrantly connected task-independent brain networks in children who have experienced severe psychosocial deprivation. Considering these networks' potential involvement in cognitive processing, including memory, visuomotor learning, visual processing, social communication, and language, these findings suggest that early psychosocial neglect associated with institutionalization may have profound adverse effects on the brain's wiring and communication, which may not be fully

reversible, at least not within a few years from the intervention. Nevertheless, statistical differences between the CAUG and FCG also suggest significant positive effects of foster care on improving neural information processing facilitated by these networks.

#### APPENDIX

The following tables provide additional information on I) the characteristics of the cohort analyzed in the study (Table A1), particularly the summary statistics of time spent at institutions for the three groups, at 42 and 96 mo; and 2) summary statistics (median and quartiles) of estimated oscillation frequencies for the three groups, at the four assessment ages (Table A2). Dominant oscillation frequencies in infants and children do not typically fall within the adult ranges of established biological bands. Therefore, these estimates and their age-related changes provide a more appropriate range of oscillation frequencies at each assessment age. Tables A3, A4, A5, A6, and A7 provide the statistical regression model parameters (regression coefficient, CI for this coefficient, standard error, P value, and Wald statistic) for each network parameter [edge connectivity (measured by mutual information) and node connectedness/strength], for each estimated oscillation. Tables A6 and A7 provide information on mixed effects regression models, which were developed to assess the trajectories, i.e., age-related changes in these network parameters from 42 to 96 mo.

Table A2. Characteristic oscillation frequency summary statistics (medians and (25th, 75th) quartiles) for each group at each assessment age

		Care a	s Usual Group	Foste	er Care Group	Never-Institutionalized Group	
Age, mo	Band Range	Median (Hz)	(25th, 75th) quartiles	Median (Hz)	(25th, 75th) quartiles	Median (Hz)	(25th, 75th) quartiles
Baseline (< 30)	Gamma	51.82	(49.93, 53.65)	50.89	(49.71, 51.82)	49.12	(48.21, 50.35)
	Beta	20.57	(19.27, 21.30)	20.18	(19.58, 20.89)	19.82	(18.87, 20.21)
	Alpha	8.24	(7.85, 8.58)	8.23	(7.96, 8.56)	8.14	(7.87, 8.45)
	Theta	3.55	(3.42, 3.69)	3.61	(3.43, 3.70)	3.61	(3.46, 3.72)
	Delta	1.54	(1.46, 1.59)	1.56	(1.47, 1.61)	1.56	(1.50, 1.61)
30–33	Gamma	50.14	(48.41, 52.47)	51.34	(48.84, 53.69)	50.01	(48.44, 53.24)
	Beta	19.94	(18.79, 21.11)	20.47	(19.39, 21.70)	19.78	(18.55, 21.47)
	Alpha	8.20	(7.73, 8.64)	8.43	(7.92, 8.88)	8.28	(7.86, 8.82)
	Theta	3.60	(3.40, 3.79)	3.66	(3.42, 3.95)	3.64	(3.47, 3.85)
	Delta	1.54	(1.45, 1.63)	1.58	(1.49, 1.72)	1.60	(1.51, 1.64)
42	Gamma	52.96	(50.16, 55.25)	53.55	(50.59, 56.54)	53.14	(48.20, 56.59
	Beta	20.58	(19.46, 22.01)	21.47	(19.70, 22.62)	21.34	(18.56, 22.88)
	Alpha	8.54	(8.13, 9.04)	8.69	(8.30, 9.32)	8.81	(8.17, 9.58)
	Theta	3.71	(3.56, 3.96)	3.82	(3.58, 4.14)	3.90	(3.62, 4.25)
	Delta	1.60	(1.52, 1.70)	1.65	(1.51, 1.80)	1.69	(1.56, 1.83)
96	Gamma	55.54	(53.19, 57.20)	54.34	(52.25, 55.83)	55.10	(53.26, 56.37)
	Beta	20.25	(19.43, 21.16)	20.13	(19.31, 20.86)	19.81	(18.93, 21.08)
	Alpha	8.43	(8.15, 8.76)	8.28	(8.06, 8.63)	8.45	(8.05, 8.82)
	Theta	3.67	(3.56, 3.81)	3.66	(3.53, 3.83)	3.74	(3.60, 3.90)
	Delta	1.61	(1.53, 1.66)	1.58	(1.53, 1.65)	1.61	(1.55, 1.69)

Table A3. Summary of statistics for linear regression models for pairwise connectivities at 96 mo as a function of group with an adjustment for birth weight or head circumference at that age

Node Pair	Median Mutual Information (CAUG, FCG, NIG)	Regression Coefficient	Confidence Interval	Standard Error	P Value	Wald Statistic
		Commo Ossill	ation Connectivity			
(P3, Pz)	0.096, 0.084, 0.073	-0.009	[-0.017, -5E-04]	0.004	0.037	4.44
(P4, O1)	0.024, 0.018, 0.014	-0.005	[-0.009, -3E-04]	0.004	0.037	4.40
(P4, O2)	0.059, 0.048, 0.040	-0.009	[-0.014, -0.003]	0.002	0.002	9.66
(Pz, O1)	0.051, 0.042, 0.036	-0.009 $-0.006$	[-0.014, -0.003] [-0.012, -0.002]	0.003	0.002	7.27
(Pz, O1) (Pz, O2)	0.053, 0.042, 0.036	-0.000 $-0.007$	[-0.012, -0.002] [-0.012, -0.002]	0.003	0.008	7.58
Network	0.054, 0.044, 0.057	-0.007 $-0.007$	[-0.012, -0.002] [-0.011, -0.003]	0.003	0.007	9.76
Network	0.034, 0.048, 0.041			0.001	0.002	9.70
(F2 F4)	0.020.0.024.0.047		ion Connectivity	0.002	0.042	4.25
(F3, F4)	0.028, 0.034, 0.047	0.005	[2.00E-04, 0.009]	0.002	0.042	4.25
(F3, T7)	0.016, 0.021, 0.031	0.005	[0.002, 0.009]	0.002	0.005	8.32
(F4, T7)	0.005, 0.009, 0.013	0.003	[0.001, 0.005]	0.001	0.002	9.83
(Fz, T7)	0.006, 0.010, 0.015	0.003	[0.001, 0.005]	9.20E-004	0.002	10.02
(C4, T7)	0.003, 0.005, 0.010	0.001	[1.00E-04, 0.003]	6.30E-004	0.030	4.82
(P3, Pz)	0.115, 0.096, 0.080	-0.008	[-0.014, -0.002]	0.003	0.016	5.98
(P3, T7)	0.018, 0.027, 0.035	0.004	[4.00E-04, 0.007]	0.002	0.030	4.86
(T7, T8)	0.008, 0.012, 0.019	0.004	[0.001, 0.007]	0.001	0.004	8.60
(T7, O1)	0.010, 0.017, 0.029	0.005	[0.001, 0.009]	0.002	0.008	7.23
(T7, O2)	0.008, 0.012, 0.022	0.004	[5.00E-04, 0.007]	0.002	0.023	5.36
Network	0.012, 0.016, 0.021	0.003	[5.00E-04, 0.006]	0.001	0.021	5.44
		Alpha Oscilla	tion Connectivity			
(F3, T7)	0.038, 0.047, 0.059	0.005	[3.00E-04, 0.009]	0.002	0.036	4.50
(F4, T7)	0.022, 0.028, 0.036	0.004	[3.00E-04, 0.007]	0.002	0.031	4.78
(Fz, T7)	0.021, 0.028, 0.035	0.004	[4.00E-04, 0.007]	0.002	0.029	4.89
(P3, Pz)	0.087, 0.073, 0.063	-0.007	[-0.011, -0.002]	0.002	0.009	6.99
(P4, Pz)	0.076, 0.067, 0.057	-0.005	[-0.010, -3.0E-04]	0.002	0.036	4.52
(P4, O2)	0.070, 0.062, 0.053	-0.005	[-0.009, -0.001]	0.002	0.012	6.56
(T7, O1)	0.026, 0.040, 0.051	0.005	[9.00E-04, 0.009]	0.002	0.018	5.76
(T7, O2)	0.021, 0.027, 0.037	0.005	[0.001, 0.009]	0.002	0.013	6.37
Network	0.022, 0.029, 0.038	0.004	[7.00E-04, 0.007]	0.001	0.017	5.9
		Theta Oscilla	tion Connectivity			
(Fz, Pz)	0.011, 0.010, 0.008	-0.001	[-0.0025,-2.0E-04]	5.70E-04	0.024	5.21
(Fz, T7)	0.019, 0.022, 0.027	0.002	[2.0E-04, 0.005]	0.001	0.031	4.80
(C3, P3)	0.047, 0.041, 0.035	-0.004	[-0.008, -3.0E-04]	0.002	0.032	4.71
(C4, P4)	0.046, 0.040, 0.035	-0.003	[-0.006, -2.0E-04]	0.001	0.036	4.53
(P3, P4)	0.059, 0.053, 0.047	-0.003	[-0.006, -3.0E-04]	0.001	0.030	4.80
(P3, Pz)	0.088, 0.081, 0.073	-0.005	[-0.009, -4.0E-04]	0.002	0.032	4.73
(P4, O1)	0.051, 0.043, 0.037	-0.004	[-0.007, -7.0E-04]	0.002	0.016	5.94
(P4, O2)	0.073, 0.063, 0.056	-0.007	[-0.007, 7.02.04]	0.002	0.003	9.28
(T7, T8)	0.035, 0.041, 0.050	0.004	[4.0E-04, 0.008]	0.002	0.027	4.98
(O1, O2)	0.118, 0.104, 0.097	-0.006	[-0.012, -6.0E-04]	0.002	0.031	4.78
Network	0.048, 0.043, 0.040	-0.002	[0.013, -7.0E-04]	9.0E-04	0.043	4.20

Only the statistics for pairs of nodes with statistically distinct connectivity (edge) among 3 groups are shown, as well as averaged connectivity over the subnetwork defined by these nodes/edge pairs. Median mutual information values for each group are provided in column 2.

#### **GRANTS**

This study was supported in part by NIH Grant R01MH091363 (C. A. Nelson) and NSF BRAIN EAGER Grant 1451480 (C. Stamoulis).

#### DISCLOSURES

No conflicts of interest, financial or otherwise, are declared by the authors.

## **AUTHOR CONTRIBUTIONS**

C.H.Z., N.A.F., and C.A.N. conceived and designed research; C.S. and R.E.V. analyzed data; C.S., C.H.Z., N.A.F., and C.A.N. interpreted results of experiments; C.S. prepared figures; C.S., R.E.V., and C.A.N. drafted manuscript; C.S., R.E.V., C.H.Z., N.A.F., and C.A.N. edited and revised manuscript; C.S., R.E.V., C.H.Z., N.A.F., and C.A.N. approved final version of manuscript; C.H.Z. and N.A.F. performed experiments.

### REFERENCES

Barttfeld P, Uhrig L, Sitt JD, Sigman M, Jarraya B, Dehaene S. Signature of consciousness in the dynamics of resting-state brain activity. *Proc Natl Acad Sci USA* 112: 887–892, 2015. doi:10.1073/pnas.1418031112.

Bauer PM, Hanson JL, Pierson RK, Davidson RJ, Pollak SD. Cerebellar volume and cognitive functioning in children who experienced early deprivation. *Biol Psychiatry* 66: 1100–1106, 2009. doi:10.1016/j.biopsych.2009. 06.014.

**Bertrand O, Tallon-Baudry C.** Oscillatory gamma activity in humans: a possible role for object representation. *Int J Psychophysiol* 38: 211–223, 2000. doi:10.1016/S0167-8760(00)00166-5.

**Bick J, Zeanah CH, Fox NA, Nelson CA.** Memory and executive functioning in 12-year-old children with histories of institutional rearing. *Child Dev.* In press. doi:10.1111/cdev.12952.

Bick J, Zhu T, Stamoulis C, Fox NA, Zeanah C, Nelson CA. Effect of early institutionalization and foster care on long-term white matter development: a randomized clinical trial. *JAMA Pediatr* 169: 211–219, 2015. doi:10.1001/jamapediatrics.2014.3212.

Bluhm RL, Miller J, Lanius RA, Osuch EA, Boksman K, Neufeld RW, Théberge J, Schaefer B, Williamson P. Spontaneous low-frequency fluctuations in the BOLD signal in schizophrenic patients: anomalies in the default network. *Schizophr Bull* 33: 1004–1012, 2007. doi:10.1093/schbul/sbm052

Bos KJ, Fox N, Zeanah CH, Nelson CA III. Effects of early psychosocial deprivation on the development of memory and executive function. Front Behav Neurosci 3: 16, 2009. doi:10.3389/neuro.08.016.2009.

Table A4. Summary of statistics for linear regression models node connectedness (centrality based on the total number of connections), for each oscillation network at 42 and 96 mo

Node	Median Node Centrality (CAUG, FCG, NIG)	Regression Coefficient	Confidence Interval	Standard Error	P Value	Walt Statistic
			42 mo			
		Commo Osoil	ation Node Connectedness			
Т7	0.50, 0.42, 0.17	-0.117	[-0.187, -0.047]	0.035	0.001	10.89
1 /	0.30, 0.42, 0.17			0.055	0.001	10.69
			tion Node Connectedness			
Fz	0.50, 0.42, 0.33	-0.086	[-0.153, -0.019]	0.034	0.012	6.41
T7	0.67, 0.50, 0.33	-0.115	[-0.192, -0.039]	0.039	0.003	9.00
T8	0.67, 0.42, 0.17	-0.078	[-0.152, -0.004]	0.038	0.040	4.28
		Alpha Oscilla	ation Node Connectedness			
Pz	0.67, 0.50, 0.42	-0.078	[-0.143, -0.014]	0.033	0.018	5.75
		Thata Oscilla	tion Node Connectedness			
Fz	0.50, 0.33, 0.25	-0.092	[-0.152, -0.033]	0.030	0.002	9.56
Pz	0.58, 0.50, 0.42	-0.101	[-0.165, -0.037]	0.030	0.002	9.77
ΓZ	0.38, 0.30, 0.42	-0.101		0.032	0.002	9.11
			96 mo			
			lation Node Connectedness			
Pz	0.50, 0.42, 0.33	-0.080	[-0.149, -0.011]	0.035	0.024	5.23
		Beta Oscilla	tion Node Connectedness			
Pz	0.58, 0.5, 0.42	-0.094	[-0.156, -0.033]	0.031	0.003	9.22
T7	0.08, 0.17, 0.25	0.079	[0.016, 0.142]	0.032	0.015	6.09
	, ,	Alpha Osaille	ntion Node Connectedness			
C3	0.50, 0.33, 0.25	-0.089	[-0.162, -0.016]	0.037	0.017	5.87
C4	0.42, 0.33, 0.17	-0.089 $-0.082$	[-0.162, -0.016] [-0.152, -0.013]	0.037	0.017	5.48
P4	0.42, 0.33, 0.17	-0.062 $-0.068$	[-0.132, -0.013] [-0.134, -0.001]	0.033	0.021	4.00
Pz	0.58, 0.42, 0.33	-0.008 $-0.083$	[-0.134, -0.001] [-0.147, -0.020]	0.034	0.047	6.68
T7	0.38, 0.42, 0.33	0.070	[0.001, 0.140]	0.032	0.011	3.98
1 /	0.17, 0.42, 0.30		. , ,	0.055	0.048	3.98
			tion Node Connectedness			
Fz	0.42, 0.33, 0.25	-0.077	[-0.135, -0.018]	0.030	0.011	6.58
C3	0.50, 0.42, 0.33	-0.085	[-0.158, -0.012]	0.037	0.022	5.32
C4	0.42, 0.33, 0.25	-0.070	[-0.140, -0.001]	0.035	0.047	4.00
P4	0.50, 0.42, 0.33	-0.067	[-0.130, -0.005]	0.032	0.035	4.51
Pz	0.58, 0.50, 0.33	-0.094	[-0.160, -0.030]	0.033	0.005	8.28

Only the statistics for the Group parameter are shown, for nodes that were statistically distinct in the 3 groups when adjusted for birth weight or head circumference. Median connectedness values for each group are provided in column 2.

Table A5. Summary of statistics for linear regression models node strength (centrality based on the sum of node weights), for each gamma, beta, alpha, and theta networks at 96 mo

Node	Median Node Centrality pqa(CAUG, FCG, NIG)	Regression Coefficient	Confidence Interval	Standard Error	P Value	Walt Statistic
		Gamma Os	scillation Node Strength			
Pz	0.1165, 0.1091, 0.1032	-0.004	[-0.008, -7E-04]	0.002	0.048	3.99
		Beta Osc	illation Node Strength			
F3	0.1019, 0.1037, 0.1056	0.002	[1E-04, 0.004]	0.001	0.034	4.63
F4	0.1005, 0.1024, 0.1047	0.002	[3E-04, 0.004]	0.001	0.019	5.69
Fz	0.1007, 0.1021, 0.1038	0.001	[1E-04, 0.003]	0.001	0.036	4.51
Pz	0.1122, 0.1106, 0.1084	-0.002	[-0.004, -1E-04]	0.001	0.048	3.99
T7	0.0943, 0.0974, 0.1011	0.003	[0.001, 0.005]	0.001	0.002	10.55
		Alpha Oso	cillation Node Strength			
P4	0.1146, 0.1100, 0.1061	-0.002	[-0.003, -1E-04]	0.001	0.041	4.28
Pz	0.1125, 0.1084, 0.1050	-0.002	[-0.003, -9E-05]	0.001	0.050	3.84
T7	0.1095, 0.1123, 0.1146	0.003	[2E-04, 0.005]	0.001	0.038	4.40
		Theta Osc	cillation Node Strength			
P4	0.1173, 0.1151, 0.1139	-0.002	[-0.003, -4E-04]	0.001	0.012	6.49
T7	0.1067, 0.1104, 0.1143	0.002	[1E-04, 0.004]	0.001	0.040	4.33

Only the statistics for nodes that were statistically distinct in the 3 groups when adjusted for birth weight or head circumference are shown. Median node strength values for each group are provided in column 2.

Table A6. Summary of linear mixed effects regression models statistics for pairwise connectivity trajectories from 42 to 96 mo, as a function of time and group, adjusted for birth weight and/or head circumference

Node pair	Regression Coefficient	Confidence Interval	Standard Error	P Value	Walt Statistic
		Gamma Oscillation Conne	ectivity (Network Edge) Traj	ectory	
(C3, P3)	-0.016	[-0.030, -0.002]	0.007	0.024	5.13
(P3, Pz)	-0.019	[-0.033, -0.005]	0.007	0.007	7.29
(P3, O2)	-0.012	[-0.023, -0.001]	0.006	0.029	4.80
(P4, O1)	-0.011	[-0.022, -0.001]	0.005	0.032	4.65
(P4, O2)	-0.014	[-0.025, -0.003]	0.006	0.014	6.10
(Pz, O2)	-0.011	[-0.022, -0.001]	0.005	0.031	4.69
		Beta Oscillation Connec	tivity (Network Edge) Trajec	ctory	
(P3, Pz)	-0.005	[-0.011, -1E-04]	0.003	0.050	3.80
		Alpha Oscillation Connec	ctivity (Network Edge) Traje	ctory	
(P3, Pz)	-0.006	[-0.011, -0.001]	0.003	0.049	3.90
(P4, O2)	-0.006	[-0.011, -0.001]	0.003	0.05	3.89
		Theta Oscillation Connec	ctivity (Network Edge) Traje	ctory	
(P3, Pz)	-0.008	[-0.012, -0.002]	0.002	0.015	6.03
(P4, O2)	-0.007	[-0.012, -0.002]	0.002	0.010	6.82

Only the statistics for the Group parameter are shown, for pairs of nodes for which their connectivity (edge) was statistically distinct in the 3 groups.

Buckner RL, Andrews-Hanna JR, Schacter DL. The brain's default network: anatomy, function, and relevance to disease. *Ann N Y Acad Sci* 1124: 1–38, 2008. doi:10.1196/annals.1440.011.

**Buckner RL, Carroll DC.** Self-projection and the brain. *Trends Cogn Sci* 11: 49–57, 2007. doi:10.1016/j.tics.2006.11.004.

Bullmore E, Sporns O. Complex brain networks: graph theoretical analysis of structural and functional systems. *Nat Rev Neurosci* 10: 186–198, 2009. doi:10.1038/nrn2575.

Cabeza R, Ciaramelli E, Olson IR, Moscovitch M. The parietal cortex and episodic memory: an attentional account. *Nat Rev Neurosci* 9: 613–625, 2008. doi:10.1038/nrn2459.

Carlqvist H, Nikulin VV, Strömberg JO, Brismar T. Amplitude and phase relationship between alpha and beta oscillations in the human electroencephalogram. *Med Biol Eng Comput* 43: 599–607, 2005. doi:10.1007/ BF02351033.

Chella F, Pizzella V, Zappasodi F, Marzetti L. Impact of the reference choice on scalp EEG connectivity estimation. J Neural Eng 13: 036016, 2016. doi:10.1088/1741-2560/13/3/036016.

Chugani HT, Behen ME, Muzik O, Juhász C, Nagy F, Chugani DC. Local brain functional activity following early deprivation: a study of postinstitutionalized Romanian orphans. *Neuroimage* 14: 1290–1301, 2001. doi:10. 1006/nimg.2001.0917.

Cover TM, Thomas JA. Elements of Information Theory (2nd ed.). Hoboken, NJ: Wiley, 2006.

Croft C, Beckett C, Rutter M, Castle J, Colvert E, Groothues C, Hawkins A, Kreppner J, Stevens SE, Sonuga-Barke EJ. Early adolescent outcomes of institutionally-deprived and non-deprived adoptees. II: language as a protective factor and a vulnerable outcome. *J Child Psychol Psychiatry* 48: 31–44, 2007. doi:10.1111/j.1469-7610.2006.01689.x.

**Dien J.** Issues in the application of the average reference: review, critiques, and recommendations. *Behav Res Methods Instrum Comput* 30: 34–43, 1998. doi:10.3758/BF03209414.

Dosenbach NU, Fair DA, Cohen AL, Schlaggar BL, Petersen SE. A dual-networks architecture of top-down control. *Trends Cogn Sci* 12: 99– 105, 2008. doi:10.1016/j.tics.2008.01.001. Efron B, Tibshirani R. An Introduction to the Bootstrap. New York: Chapman and Hall, 1993. doi:10.1007/978-1-4899-4541-9.

Eluvathingal TJ, Chugani HT, Behen ME, Juhász C, Muzik O, Maqbool M, Chugani DC, Makki M. Abnormal brain connectivity in children after early severe socioemotional deprivation: a diffusion tensor imaging study. *Pediatrics* 117: 2093–2100, 2006. doi:10.1542/peds.2005-1727.

Fair DA, Cohen AL, Dosenbach NU, Church JA, Miezin FM, Barch DM, Raichle ME, Petersen SE, Schlaggar BL. The maturing architecture of the brain's default network. *Proc Natl Acad Sci USA* 105: 4028–4032, 2008. doi:10.1073/pnas.0800376105.

Fox MD, Snyder AZ, Vincent JL, Corbetta M, Van Essen DC, Raichle ME. The human brain is intrinsically organized into dynamic, anti-correlated functional networks. *Proc Natl Acad Sci USA* 102: 9673–9678, 2005. doi:10.1073/pnas.0504136102.

Fransson P, Skiöld B, Horsch S, Nordell A, Blennow M, Lagercrantz H, Aden U. Resting-state networks in the infant brain. *Proc Natl Acad Sci USA* 104: 15531–15536, 2007. doi:10.1073/pnas.0704380104.

**Galletti C, Kutz DF, Gamberini M, Breveglieri R, Fattori P.** Role of the medial parieto-occipital cortex in the control of reaching and grasping movements. *Exp Brain Res* 153: 158–170, 2003. doi:10.1007/s00221-003-1589-z.

**Gelman A, Hill J, Yajima M.** Why we (usually) don't have to worry about multiple comparisons. *J Res Educ Eff* 5: 189–211, 2012. doi:10.1080/19345747.2011.618213.

**Greicius MD, Krasnow B, Reiss AL, Menon V.** Functional connectivity in the resting brain: a network analysis of the default mode hypothesis. *Proc Natl Acad Sci USA* 100: 253–258, 2003. doi:10.1073/pnas.0135058100.

**Greicius MD, Supekar K, Menon V, Dougherty RF.** Resting-state functional connectivity reflects structural connectivity in the default mode network. *Cereb Cortex* 19: 72–78, 2009. doi:10.1093/cercor/bhn059.

Helfrich RF, Knepper H, Nolte G, Strüber D, Rach S, Herrmann CS, Schneider TR, Engel AK. Selective modulation of interhemispheric functional connectivity by HD-tACS shapes perception. *PLoS Biol* 12: e1002031, 2014. doi:10.1371/journal.pbio.1002031.

Table A7. Summary of linear mixed effects regression models statistics for the trajectories of node connectedness from 42 to 96 mo, as a function of time and group, adjusted for birth weight and/or head circumference

Node	Regression Coefficient	Confidence Interval	Standard Error	P Value	Walt Statistic
		Alpha Oscillation N	ode Connectedness Trajectory		
P4	-0.053	[-0.088, -0.017]	0.018	0.004	8.60
Pz	-0.035	[-0.066, -0.003]	0.016	0.030	4.77
		Theta Oscillation No	ode Connectedness Trajectory		
P4	-0.045	[-0.087, -0.003]	0.021	0.036	4.44
Pz	-0.040	[-0.073, -0.007]	0.017	0.018	5.71

Only the statistics for the Group parameter are shown, for pairs of nodes that were statistically distinct in the 3 groups.

- Huang NE, Shen Z, Long SR, Wu MC, Shih HH, Zheng Q, Yen NC, Tung CC, Liu HH. The empirical mode decomposition and the Hilbert spectrum for nonlinear and non-stationary time series analysis. *Proc Royal Soc A* 454: 903–995, 1998. doi:10.1098/rspa.1998.0193.
- Kelly AM, Uddin LQ, Biswal BB, Castellanos FX, Milham MP. Competition between functional brain networks mediates behavioral variability. *Neuroimage* 39: 527–537, 2008. doi:10.1016/j.neuroimage.2007.08.008.
- **Kennedy DP, Redcay E, Courchesne E.** Failing to deactivate: resting functional abnormalities in autism. *Proc Natl Acad Sci USA* 103: 8275–8280, 2006. doi:10.1073/pnas.0600674103.
- Konrad K, Eickhoff SB. Is the ADHD brain wired differently? A review on structural and functional connectivity in attention deficit hyperactivity disorder. *Hum Brain Mapp* 31: 904–916, 2010. doi:10.1002/hbm.21058.
- **Lauritzen TZ, D'Esposito M, Heeger DJ, Silver MA.** Top-down flow of visual spatial attention signals from parietal to occipital cortex. *J Vis* 9: 18, 2009. doi:10.1167/9.13.18.
- Mantini D, Perrucci MG, Del Gratta C, Romani GL, Corbetta M. Electrophysiological signatures of resting state networks in the human brain. *Proc Natl Acad Sci USA* 104: 13170–13175, 2007. doi:10.1073/pnas. 0700668104
- Marshall PJ, Fox NA; Bucharest Early Intervention Project Core Group. A comparison of the electroencephalogram between institutionalized and community children in Romania. *J Cogn Neurosci* 16: 1327–1338, 2004. doi:10.1162/0898929042304723.
- Marshall PJ, Reeb BC, Fox NA, Nelson CA III, Zeanah CH. Effects of early intervention on EEG power and coherence in previously institutionalized children in Romania. *Dev Psychopathol* 20: 861–880, 2008. doi:10.1017/S0954579408000412.
- McLaughlin KA, Fox NA, Zeanah CH, Nelson CA. Adverse rearing environments and neural development in children: the development of frontal electroencephalogram asymmetry. *Biol Psychiatry* 70: 1008–1015, 2011. doi:10.1016/j.biopsych.2011.08.006.
- McLaughlin KA, Fox NA, Zeanah CH, Sheridan MA, Marshall P, Nelson CA. Delayed maturation in brain electrical activity partially explains the association between early environmental deprivation and symptoms of attention-deficit/hyper-activity disorder. *Biol Psychiatry* 68: 239–336, 2010. doi:10.1016/j.biopsych.2010.04.005.
- Nelson CA, Fox NA, Zeanah CH. Romania's Abandoned Children: Deprivation, Brain Development and the Struggle for Recovery. Cambridge, MA: Harvard University Press, 2014.
- Nelson CA, de Haan M, Thomas KM. Neuroscience of Cognitive Development: The Role of Experience and the Developing Brain. New York, NY: Wiley, 2006.
- Palus M, Komárek V, Procházka T, Hrncír Z, Sterbová K. Synchronization and information flow in EEGs of epileptic patients. *IEEE Eng Med Biol Mag* 20: 65–71, 2001. doi:10.1109/51.956821.
- Papoutsi M, Stamatakis EA, Griffiths J, Marslen-Wilson WD, Tyler LK. Is left fronto-temporal connectivity essential for syntax? Effective connectivity, tractography and performance in left-hemisphere damaged patients. *Neuroimage* 58: 656–664, 2011. doi:10.1016/j.neuroimage.2011.06.036.
- Perfetti B, Moisello C, Landsnesors EC, Kvint S, Lanzafame S, Onofri M, Di Rocco A, Tononi G, Ghilardi MF. Modulation of gamma and theta spectral amplitude and phase synchronization is associated with the development of visuo-motor learning. *J Neurosci* 31: 14810–14819, 2011. doi: 10.1523/JNEUROSCI.1319-11.2011.
- Pollak S, Nelson CA, Schlaak MF, Roeber BJ, Wewerka SS, Wiik KL, Frenn KA, Loman MM, Gunnar MR. Neurodevelopmental effects of early deprivation in post-institutionalized children. *Child Dev* 81: 224–236, 2010. doi:10.1111/j.1467-8624.2009.01391.x.
- Raichle ME, MacLeod AM, Snyder AZ, Powers WJ, Gusnard DA, Shulman GL. A default mode of brain function. *Proc Natl Acad Sci USA* 98: 676–682, 2001. doi:10.1073/pnas.98.2.676.
- **Raichle ME, Snyder AZ.** A default mode of brain function: a brief history of an evolving idea. *Neuroimage* 37: 1083–1090, 2007. doi:10.1016/j. neuroimage.2007.02.041.
- Schreiber T. Measuring information transfer. Phys Rev Lett 85: 461–464, 2000. doi:10.1103/PhysRevLett.85.461.
- Sheridan MA, Fox NA, Zeanah CH, McLaughlin KA, Nelson CA III. Variation in neural development as a result of exposure to institutionalization early in childhood. *Proc Natl Acad Sci USA* 109: 12927–12932, 2012. doi:10.1073/pnas.1200041109.

- **Stamoulis C, Betensky RA.** A novel signal processing approach for the detection of copy number variations in the human genome. *Bioinformatics* 27: 2338–2345, 2011. doi:10.1093/bioinformatics/btr402.
- Stamoulis C, Chang BS. Application of matched-filtering to extract EEG features and decouple signal contributions from multiple seizure foci in brain malformations. *IEEE Proc 4th International IEEE/EBMS Conf Neural Eng* 2009: 514–517, 2009. doi:10.1109/NER.2009.5109346.
- **Stamoulis C, Schomer DL, Chang BS.** Information theoretic measures of network coordination in high-frequency scalp EEG reveal dynamic patterns associated with seizure termination. *Epilepsy Res* 105: 299–315, 2013. doi:10.1016/j.eplepsyres.2013.03.001.
- **Stamoulis C, Vanderwert RE, Zeanah CH, Fox NA, Nelson CA.** Early psychosocial neglect adversely impacts developmental trajectories of brain oscillations and their interactions. *J Cogn Neurosci* 27: 2512–2528, 2015. doi:10.1162/jocn a 00877.
- Stamoulis C, Vogel-Farley V, Degregorio G, Jeste SS, Nelson CA. Resting and task-modulated high-frequency brain rhythms measured by scalp encephalography in infants with tuberous sclerosis complex. *J Autism Dev Disord* 45: 336–353, 2015. doi:10.1007/s10803-013-1887-7.
- **Tallon-Baudry C.** The roles of gamma-band oscillatory synchrony in human visual cognition. *Front Biosci (Landmark Ed)* 14: 321–332, 2009. doi:10. 2741/3246.
- **Tomasi D, Volkow ND.** Association between functional connectivity hubs and brain networks. *Cereb Cortex* 21: 2003–2013, 2011. doi:10.1093/cercor/bhq268.
- Tosoni A, Pitzalis S, Committeri G, Fattori P, Galletti C, Galati G. Resting-state connectivity and functional specialization in human medial parieto-occipital cortex. *Brain Struct Func* 220: 3307–3321, 2015. doi:10.1007/s00429-014-0858-x.
- **Tottenham N, Hare TA, Millner A, Gilhooly T, Zevin JD, Casey BJ.** Elevated amygdala response to faces following early deprivation. *Dev Sci* 14: 190–204, 2011. doi:10.1111/j.1467-7687.2010.00971.x.
- Tukey JW. Exploratory Data Analysis. Reading, MA: Addison-Wesley, 1977.
   Tyler LK, Marslen-Wilson WD, Randall B, Wright P, Devereux BJ,
   Zhuang J, Papoutsi M, Stamatakis EA. Left inferior frontal cortex and syntax: function, structure and behaviour in patients with left hemisphere damage. Brain 134: 415–431, 2011. doi:10.1093/brain/awq369.
- Vanderwert RE, Marshall PJ, Nelson CA III, Zeanah CH, Fox NA. Timing of intervention affects brain electrical activity in children exposed to severe psychosocial neglect. *PLoS One* 5: e11415, 2010. doi:10.1371/journal.pone. 0011415.
- Vejmelka M, Palus M. Inferring the directionality of coupling with conditional mutual information. *Phys Rev E Stat Nonlin Soft Matter Phys* 77: 026214, 2008. doi:10.1103/PhysRevE.77.026214.
- Vicente R, Wibral M, Lindner M, Pipa G. Transfer entropy—a model-free measure of effective connectivity for the neurosciences. *J Comput Neurosci* 30: 45–67, 2011. doi:10.1007/s10827-010-0262-3.
- Vincent JL, Snyder AZ, Fox MD, Shannon BJ, Andrews JR, Raichle ME, Buckner RL. Coherent spontaneous activity identifies a hippocampal-parietal memory network. *J Neurophysiol* 96: 3517–3531, 2006. doi:10. 1152/jn.00048.2006.
- Ward AM, Schultz AP, Huijbers W, Van Dijk KR, Hedden T, Sperling RA. The parahippocampal gyrus links the default-mode cortical network with the medial temporal lobe memory system. *Hum Brain Mapp* 35: 1061–1073, 2014. doi:10.1002/hbm.22234.
- Windsor J, Benigno JP, Wing CA, Carroll PJ, Koga SF, Nelson CA III, Fox NA, Zeanah CH. Effect of foster care on young children's language learning. *Child Dev* 82: 1040–1046, 2011. doi:10.1111/j.1467-8624. 2011.01604.x.
- Windsor J, Moraru A, Nelson CA, Fox NA, Zeanah CH. Effect of foster care on language learning at eight years: findings from the Bucharest Early Intervention Project. J Child Lang 40: 605–627, 2013. doi:10.1017/ S0305000912000177.
- Wu Z, Huang N. Ensemble empirical mode decomposition: a noise-assisted data analysis method. Adv Adapt Data Anal 01: 1–41, 2009. doi:10.1142/ S1793536909000047.
- Zeanah CH, Nelson CA, Fox NA, Smyke AT, Marshall P, Parker SW, Koga S. Designing research to study the effects of institutionalization on brain and behavioral development: the Bucharest Early Intervention Project. *Dev Psychopathol* 15: 885–907, 2003. doi:10.1017/S0954579403000452.